Helsinki University of Technology Laboratory of Space Technology

Espoo, January 2001 REPORT 44

SNOW MONITORING USING MICROWAVE RADARS

Jarkko Koskinen

Thesis for the degree of Doctor of Technology

Snow Monitoring Using Microwave Radars

Jarkko Koskinen

Report 44

January 2001

Helsinki University of Technology

Department of Electrical and Communications Engineering

Laboratory of Space Technology

Dissertation for the degree of Doctor of Science in Technology (Doctor of Philosophy) to be presented with due permission of Department of Electrical and Communications Engineering, for public examination and debate in Auditorium S5 at Helsinki University of Technology (Espoo, Finland) on the 19th of January, 2001, at 12 o'clock noon.

ISBN 951-22-5308-9
ISSN 0786-8154

Table of Contents

Preface

This thesis has been conducted in the Laboratory of Space Technology in Helsinki University of Technology under the supervision of Professor Martti Hallikainen. The papers presented in this thesis are closely related to ESA's Announcement of Opportunity project "Application of ERS-1 Active Microwave Instrumentation Data to Remote Sensing of Snow", National "Snowmap" project and EU's "Snow-Tools" project.

I want to express my gratitude to Professor Martti Hallikainen for acting as supervisor and tutor in all of the papers and in my thesis. Especially I wish to mention Dr. Jouni Pulliainen who strongly influenced my research and papers concerning the studies with backscattering models. I want to thank Dr. Juerg Lichtenegger and Mr. Gaute Solaas for their aid during my stay in ESA-ESRIN and all the people who participated my studies and publications. I also like to thank my research group (Jaan Praks, Ali Nadir Arslan, Hanna Alasalmi and Nerius Kruopis) for helping and supporting me during this work.

I want to thank Jenny and Antti Wihuri Foundation, August and Lydia Heino Foundation and Vaisala Foundation for supporting my studies.

I am also grateful to my family for their support.

Finally, I would like to dedicate this work to my father, who always trusted me in my megalomaniac dreams.

Helsinki, 15 November 2000

Jarkko Koskinen

Abstract

Remote sensing has proven its usefulness in various applications. For mapping, land-use classification and forest monitoring optical satellite and airborne images are used operationally. However, this is not the case with snow monitoring. Currently only ground-based *in situ* and weather measurements are used operationally for snow monitoring in Finland. Ground measurements are conducted once a month on special snow courses. These measurements are used to update the hydrological model that simulates the runoff. Recently optical images (NOAA AVHRR) have been tested to derive a map of the areal extent of snow. However, during the snow melt, which is the most important period for hydrology, there are few cloudless days and, therefore, the availability of optical data is limited. That is why microwave remote sensing can play an important role in snow melt monitoring due to its unique capability to provide data independent of sun light and in almost all weather conditions. The synthetic aperture radar (SAR) data may make a significant contribution to satellite observations of snow by bridging the period between the on-set and end of snow melt. Microwave radiometers can be used to retrieve the snow water equivalent of dry snow, but they cannot be used to distinguish wet snow and wet ground during the melting period. The results of the thesis indicate that, even in the presence of forest canopies, (1) wet snow can be distinguished from dry snow and bare ground, (2) snow-free areas can be identified, (3) seasonal evolution of snow cover can be monitored and (4) snow-melt maps showing the fraction of snow-free ground (wet ground) and snow (wet snow) can be derived from SAR images.

Keywords: Remote sensing, SAR, snow monitoring, microwave backscattering modeling

List of Appended Papers

This thesis is based on the work contained in the following papers, hereafter referred to as Papers A-E:

Paper A. J. Koskinen, J. Pulliainen, M. Hallikainen, "Land-Use Classification Employing ERS-1 SAR Data", *Photogrammetric Journal of Finland*, Vol. 14, No. 2, pp. 23-34, 1995.

Paper B. J. Koskinen, J. Pulliainen, M. Hallikainen, "The Use of ERS-1 SAR Data in Snow Melt Monitoring", *IEEE Trans. on Geoscience and Remote Sensing*, Vol. 35, No. 3, pp. 601-610, 1997.

Paper C. J. Koskinen, J. Pulliainen, M. Mäkynen, M. Hallikainen, M. "Seasonal Comparison of Ranging Scatterometer and ERS-1 Microwave Signatures over Boreal Forest Zone", *IEEE Trans. on Geoscience and Remote Sensing*, Vol. 37 No. 4, pp. 2068-2079, 1999.

Paper D. J. Koskinen, S. Metsämäki, J. Grandell, S. Jänne, L. Matikainen, M. Hallikainen, "Snow Monitoring Using Radar and Optical Satellite Data", *Remote Sensing of Environment*, Vol. 69, No. 1, pp. 16-29, 1999.

Paper E. J. Koskinen, J. Pulliainen, M. Hallikainen, "Effect of Snow Wetness to C-Band Backscatter - A Modeling Approach", *Report 41 Laboratory of Space Technology, Helsinki University of Technology*, Espoo, 20 p., 2000.

The main responsibility in preparing all papers above lay on the first author.

In Paper A ERS-1 SAR data is employed for land-use classification in the Sodankylä test site, in Northern Finland. SAR data analysis, algorithm development and testing was conducted by me. The use of boreal forest semi-empirical model was done in co-operation with Dr. Jouni Pulliainen.

Paper B deals with the novel snow melt algorithm. In this paper my responsibility covered all the processing and the development of the classification algorithm with some help from Dr. Jouni Pulliainen. In addition to this paper a shorter version of the study was published in *Physics and Chemistry of the Earth*, Vol. 22, No. 3-4, pp. 285-289. The paper is based on my presentation at European Geophysical Society's conference (EGS'96) where it was selected to be published in the journal mentioned above.

In Paper C a comparison of airborne ranging scatterometer (HUTSCAT) and spaceborne SAR (ERS-1 SAR) microwave signatures is presented. The HUTSCAT processing was conducted by Mr. Marko Mäkynen, while I was responsible for SAR processing and the comparison phase. The model simulations presented in the paper were conducted by Dr. Jouni Pulliainen.

Paper D continues the research from the results presented in Paper B. In this paper combined use of ground-based *in situ* data and spaceborne SAR and optical data for snow monitoring is discussed. The optical data set was analyzed by Ms. Sari Metsämäki and Mr. Sami Jänne, the *in situ* measurements by Mr. Jochen Grandell and Ms. Leena Matikainen, while I was responsible for SAR data analysis and comparison with ground measurements.

Paper E presents a backscattering model for snow cover. The snow model is combined with the boreal forest backscattering model in order to allow snow monitoring in forested areas. This model is used to simulate the backscatter under various snow conditions and, based on these simulations, a theoretical accuracy is determined for the snow melt algorithm introduced in Papers B and D. I conducted all the modeling work and simulations, while the use of boreal forest semi-empirical model was done in co-operation with Dr. Jouni Pulliainen

1. Introduction

In remote sensing satellite and airborne instruments are used to measure the properties of land, sea and atmosphere. Remote sensing offers a possibility to cover large areas quickly and often with a low cost compared to the more traditional methods. Remote sensing is mainly used to monitor the state of the environment, to map natural resources and to improve process understanding and integration of data with those from complementary sources in modeling of our environmental processes.

In remote sensing the measurement is conducted using electromagnetic waves. Most remote sensing instruments operate in the optical, near infrared, infrared or microwave band. The response depends both on the parameters of the instrument and on the properties of the target.

The presence of snow on the ground has a significant influence on the radiative balance of the Earth surface and on the heat exchange between the surface and the atmosphere. The feedback mechanism between snow extent and atmospheric temperature tends to amplify climatic anomalies. Representation of the snow cover in present climate models is not satisfactory, because the models do not yet account for the feedback mechanism between the global snow cover and the atmosphere *(Guyenne 1995).* The seasonal snow cover is mostly limited to the Northern hemisphere, where the average snow extent during the winter months ranges from 30 to 40 million km^2. The water equivalent volume of this snow mass ranges from 2000 to 3000 km^3. In northern Europe snowfall is a substantial part of the overall precipitation; e.g. in Finland 27% of the annual average total precipitation of 621 mm is snow *(Perälä et al. 1990).* Snow is a vital water resource also in many other regions of the world and estimation of the snow water content and prediction of the expected run-off rate of snow are major inputs for hydrology and the management of water and hydro-electric power schemes *(Guyenne and Bernards 1995).* In northern regions, the snow may represent more than half of the annual runoff, setting specific demands on the models employed in managing water resources. The lack of areal values for hydrological variables is one of the most important challenges in hydrologic modeling *(Solberg et al. 1997).*

The topic of this thesis is snow monitoring in Northern Finland. However, Paper A basically discusses the seasonal behavior of backscatter for various land-use categories and, therefore, describes the effect of land-use and vegetation to snow monitoring. The SAR derived land-use information can be combined with SAR-based snow melt monitoring to increase the confidence of the snow extent estimates.

The objectives of the thesis are

- development of radar-based snow mapping techniques,
- combination of airborne and spaceborne radar in remote sensing of snow,
- combination of optical and SAR data in snow extent mapping, and

- theoretical evaluation of the accuracy of radar-based snow melt monitoring.

Chapter 2 introduces the basic aspects of remote sensing of snow with emphasis on active microwave sensors. Also the effect of vegetation to remote sensing of snow is considered. This chapter describes the development of the methodology used in the thesis and compares it to the methodology reported in literature.

In Chapter 3 the methodology used in the thesis is discussed in details and the test results are presented. Also comments on the results and suggestions for future research are given.

Chapter 4 summarizes the contents of the appended papers.

2. Radar Remote Sensing of Snow

Remote sensing provides regional characteristics of the snow cover. These values are not affected by interpolation errors as opposed to values that are estimated from ground-based gauging networks. In addition, several important hydrological variables, including snow layer wetness, are difficult to measure on site. This potentially improves the appraisal of hydrological conditions in remote areas. Remote sensing instruments provide the means for continuous monitoring of the snow cover, as successfully demonstrated *(Kuittinen 1992, Solberg et al. 1994, Paper B, Paper D).* In the future, remote sensing may have an important role in retrieving information on the snow cover. Optical and near infrared sensors are mostly used to detect snow cover. These sensors can be used under cloudless clear sky conditions. A fair estimate to the thickness of snow layer can be obtained if the snow layer is thin, but these sensors cannot provide direct knowledge of snow water equivalent or temperature (Table 1) *(Rango 1986).* Passive microwave sensors have a long history in snow monitoring. Several investigations have demonstrated the capability of multi-frequency microwave radiometer systems to locally map snow extent, snow depth and snow water equivalent (Table 1) *(Hallikainen and Jolma 1992, Mäzler 1994).* Spaceborne microwave radiometers have poor spatial resolution and they cannot discriminate wet snow from bare ground. Experiments with Seasat SAR and ERS-1 SAR data have demonstrated the capability of spaceborne SAR in snow monitoring *(Rott 1984, Koskinen et al. 1994, Piesbergen et al. 1995, Guneriussen et al. 1996, Paper B, Paper D, Nagler and Rott 1998).* A very potential application for microwave radar is snow melt monitoring because of its good capability to distinguish wet snow from bare ground (Table 1)*(Paper B, Paper D).*

Table 1. *Comparison of various frequency bands for snow monitoring (Rango 1986).*

Property	Optical/ near infrared	Infrared	Microwaves
Snow extent	Yes	yes	yes
Snow depth	fair (for shallow snow only)	poor	fair
Snow water content	fair (for shallow snow only)	poor	fair
Albedo	yes	no	no
The amount of liquid water in snow	poor	poor	yes
Temperature	no	yes	poor
All weather capability	no	no	yes
Spatial resolution	~ 10 m	~ 100 m	Passive sensors 20-150 km Active sensors ~ 30 m

2.1 Backscattering from snow-covered terrain

2.1.1 The scattering mechanisms and effective snow parameters

In general, the backscattering coefficient of snow-covered terrain consists of contributions resulting from *(Ulaby et. al 1986, Fung 1994)*:

A) backscattering from the snow-air interface,

B) volume scattering from the snow layer and

C) backscattering from the underlying ground surface.

Additionally the backscattering is affected by multiple scattering/reflection resulting from snow volume and either one or both boundaries of the snow layer. Scattering from an inhomogeneous layer above a homogeneous half space (air-snow-ground system) is shown in Figure 1.

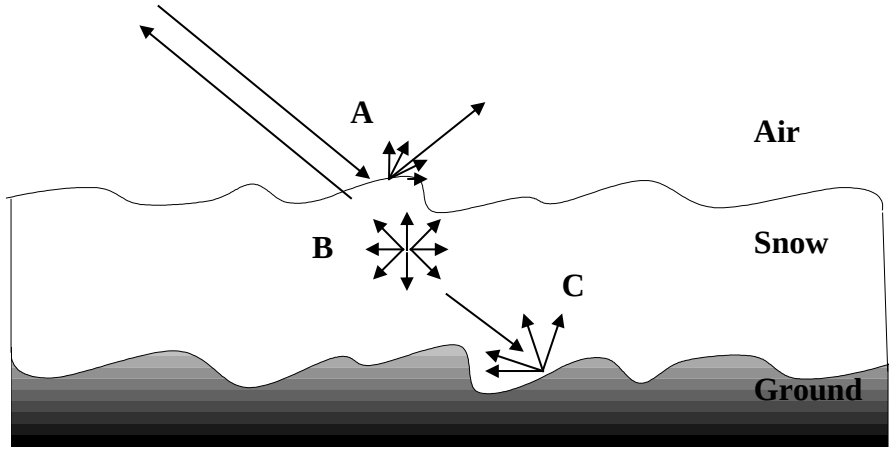

Figure 1. *Scattering mechanisms A, B and C for snow-covered terrain (see text).*

The observed backscattering coefficient is affected by several physical parameters of the snow layer. These parameters are *(Ulaby et al 1986, Pulliainen et al. 1996a)*:

- volumetric liquid water content,
- snow layer thickness,
- surface roughness (air-snow boundary and snow-ground boundary),
- snow grain size and shape (or correlation lengths),
- snow layer temperature profile,
- snow layer density profile and
- layer structure.

A commonly employed snow cover characteristic is the snow water equivalent (SWE) which is directly related to the snow layer thickness and density. The

correlation length is a parameter relevant for theoretical continuous media modeling approaches. It is related to the snow grain size and volumetric distribution of snow grains. Typically, three-dimensional correlation length information is required. In addition to characteristics mentioned above also information on the properties of vegetation characteristics (forest canopy) is required *(Pulliainen et al. 1996a).*

2.1.2 Backscattering model for snow-covered terrain

Backscattering from snow layer can be modeled by using theoretical or semi-empirical models. In theoretical backscattering model discussed here each of components A to C is approximated separately and the observed backscattering coefficient is the sum of these components. The model presented here and in Paper E is based on backscattering model introduced in (*Fung 1994).* However, this combination of the independent models has not been reported before. The terms A to C are approximated using the following backscattering models:

Term A: IEM surface scattering model (*Fung 1994),*

Term B: Volume scattering model for layers with small dielectric constant (*Fung 1994),*

Term C: Michigan Empirical Surface Scattering Model *(Oh et al. 1992).*

Additionally, a formulation to estimate the indirect contributions to the backscattering coefficient is applied (*Fung 1994).* However, the effect of indirect contributions is relatively small compared to the other backscattering contributions and, therefore, it can be neglected in most cases (*Fung 1994).*

The backscattering model is based on two major assumptions (*Fung 1994*):

- only single scattering is important,
- transmission across the top boundary can be accounted for by using the Fresnel power transmission coefficient and
- reflection at the lower boundary for the surface-volume interaction term can be calculated using the Fresnel power reflection coefficient.

More complex and accurate models that do not employ these simplifications have been introduced in the literature *(Tsang et al. 1985, Ulaby and Stiles 1986a, Fung 1994).* The main modifications in these models are the inclusion of multiple scatterers in the model and ellipsoidal and other nonspherical scatterers in the medium. However, most of these advanced models are very complicated and include parameters, which are difficult to obtain or measure.

<u>Term A: air-snow surface backscattering</u>

The air-snow boundary backscattering is approximated using the IEM surface scattering model (*Fung 1994*):

$$\sigma_A^0 = 4\pi \cos\theta_s \left[I_p(\mu_s, \phi_s) / I^i{}_p \right] \Big|_{\theta_s=\theta} = \frac{k^2}{2} \exp\left(-2k_z{}^2 \sigma_s{}^2\right) \sum_{n=1}^{\infty} \left| I^n{}_{pp} \right|^2 \frac{W^n(-2k_x, 0)}{n!} \quad (1)$$

where

$$I^n{}_{pp} = (2k_z\sigma_s)^n f_{pp} \exp\left(-2k_z{}^2\sigma_s{}^2\right) + \frac{(k_z\sigma_s)\left[F_{pp}(-k_x,0) + F_{pp}(k_x,0)\right]}{2} \quad (2)$$

and the nth power of the surface correlation function W is

$$^{(n)}(K) = \int_0^{\infty} \rho^n(\xi) J_0(K\xi) \xi d\xi = \left(\frac{L}{n}\right)^2 \left[1 + \left(\frac{KL}{n}\right)^2\right]^{-1.5} . \quad (3)$$

In Equations (1) - (3)

k	=	wave number,
K	=	normalized wave number,
k_x	=	k cos θ,
k_z	=	k sin θ,
pp	=	transmit and receive polarization,
σ_s	=	snow surface rms height,
I_{pp}	=	phase function,
J_0	=	zero-order Bessel function,
L	=	surface correlation length,
θ	=	incidence angle,
θ_s	=	reflection angle,
μ_s	=	magnetic permeability,
ξ	=	horizontal deviation,
ρ	=	correlation coefficient,
ϕ	=	azimuth angle.

Equation (3) can also be approximated with Gaussian or other exponential functions; however, according to *(Fung 1994)* this correlation function is widely used. The Gaussian function always leads to a bell-shaped correlation curve that decreases very fast for larger angles, while the exponential correlation function tends to level off *(Fung 1994).*

For the monostatic case the equations for f_{vv}, $F_{vv}(k_x,0)$ and $F_{vv}(-k_x,0)$ can be found in *(Fung 1994).* These parameters are related to the dielectric properties of snow. The dielectric properties of snow have been widely reported in the literature *(Hallikainen et al. 1986, Mätzler 1987, Denoth 1989, Mätzler 1996).*

Term B: snow volume scattering

The volume scattering portion is approximated using a volume scattering model developed for layers with a small dielectric constant *(Fung 1994).* This model applies only to point scatterers *(Fung 1994).*

$$\sigma^{0}{}_{B} = 0.5\omega \cdot T_{lt}T_{tl}\cos\theta\left[1-\exp\left(-\frac{2\tau}{\cos\theta_t}\right)\right]P_{pp}\left(\cos\theta_t,-\cos\theta_t;\pi\right), \quad (4)$$

where

ω	=	snow volume scattering albedo,
τ	=	optical depth,
P_{pp}	=	phase function of volume scattering,
T_{lt}	=	Fresnel power transmission coefficient,
θ_t	=	transmission angle.

The snow volume scattering albedo (ω) is defined as *(Ulaby et al. 1981b)*

$$\omega = \kappa_s/\kappa_e, \quad (5)$$

and the optical depth (τ) is defined as *(Ulaby et al. 1981b)*

$$\tau = \kappa_e d, \quad (6)$$

where

κ_s	=	scattering coefficient, $\kappa_s = \kappa_e - \kappa_a$,
κ_e	=	extinction coefficient,
κ_a	=	absorption coefficient, $\kappa_a = 2K\left(\left\|\mathrm{Im}\sqrt{\varepsilon_r}\right\|\right)$,
ε_r	=	relative permittivity,
d	=	snow depth.

Extinction coefficient κ_e can be modeled using MIE solution (*Ulaby et al. 1986) or* applying strong fluctuation theory *(Wang et al. 1999).*

The magnitude of the scattering coefficient κ_s depends on the size of the scatterer i.e. snow crystal size. However, it has been previously reported that when discrete particle backscattering model is used at C-band, the effective crystal size is larger than the observed mean crystal size *(Zurk et al. 1994, Kendra et al. 1998).* In this case the behavior of the target cannot be explained in terms of the particles of which the snowpack was observed. The particles must be considered as "sticky" particles, where the particles come together to form an aggregate particle, effectively much larger than the individual particles *(Zurk et al. 1994).* The authors *(Kendra et al. 1998)* found that the effective crystal size was six times larger than the observed mean crystal size at C-band.

Term C: snow-ground surface backscattering

The third term is dominated by noncoherent scattering from the bottom boundary surface attenuated by the snow layer. It is approximated by using the Michigan Empirical Surface Scattering Model *(Oh et al. 1992)* and by accounting for crossing of the top surface boundary and attenuation due to propagation loss through the layer.

$$\sigma^0{}_C = \cos(\theta) \quad T_{lt}(\theta,\theta_t) \quad T_{tl}(\theta_t,\theta) \quad \exp\left(-\frac{2\tau}{\cos\theta_t}\right) \quad \frac{\sigma^0{}_{gr}(\theta_t)}{\cos(\theta_t)}\ , \tag{7}$$

where

$$\sigma^0_{gr} = \frac{g\cdot\cos^3\theta_t}{\sqrt{p}}\cdot\left[R_v(\theta_t)+R_h(\theta_t)\right]\ , \tag{8}$$

$$\sqrt{p} = 1-\left(\frac{2\theta_t}{\pi}\right)^{\left[\frac{1}{3R_0}\right]}\cdot\exp(-k_s\sigma_g)\,, \tag{9}$$

$$g = 0.7*\left[1-\exp\left(-0.65\cdot(k_s\sigma_g)^{1.8}\right)\right]\,, \tag{10}$$

T_{pp} = Fresnel power transmission coefficient,
R_{pp} = Fresnel power reflection coefficient,
k_s = Wave number in snow
σ_g = Ground surface rms-height,
R_0 = Fresnel reflectivity of the surface at nadir, $R_0 = \left|\frac{1-\sqrt{\varepsilon_r}}{1+\sqrt{\varepsilon_r}}\right|^2$.

Indirect contributions

The indirect contribution to the backscattering coefficient is caused by the interaction between volume inhomogeneities and the lower snow-ground boundary of the layer *(Fung 1994):*

$$\begin{aligned}\sigma^0{}_D = \cos(\theta) \quad & \left(L\ T_{tl}\right)^2 L_r R_{pp}\omega \quad \left(\frac{\tau}{\cos(\theta)}\right)\cdot \\ & \left[P_{pp}(-\cos(\theta),-\cos(\theta),\phi_t,-\phi_t)+P_{pp}(\cos(\theta),\cos(\theta),\phi_t,-\phi_t)\right] \quad \exp\left(-\frac{2\tau}{\cos(\theta)}\right),\end{aligned} \tag{11}$$

where

L = Loss factor.

Figure 2 shows the behavior of the predicted backscattering components A, B and C for the backscattering model and the total backscattering coefficient at 5.3 GHz and vertical polarization as a function of snow wetness. The snow parameters used in the simulation are selected to represent the typical cases in Finland. However, the snow crystal size represents the effective snow crystal size not the observed mean crystal size. The derivation of effective snow crystal size is explained in *(Kendra et al. 1998, Paper E).*

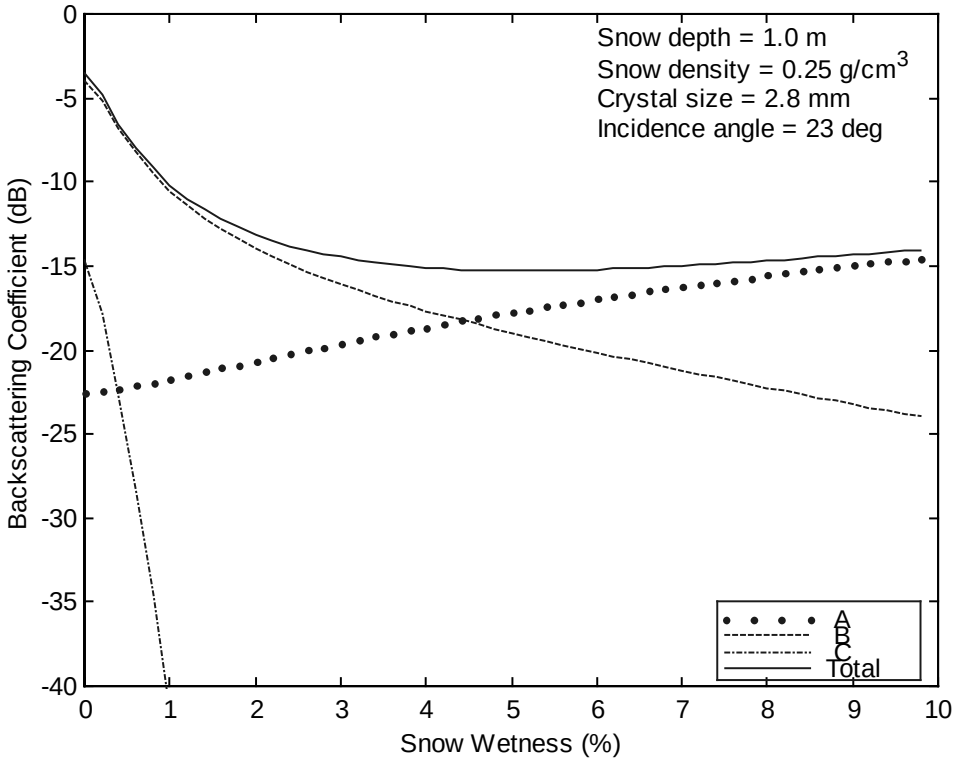

Figure 2. *Computed contribution of the components (A) snow surface backscattering, (B) snow volume scattering and (C) ground backscattering of the backscattering model and the total backscattering coefficient as a function of snow wetness (snow surface rms height (σ_s) = 0.4 cm, snow surface correlation length (l) = 5.0 cm, ground surface rms height (σ_g) = 1.2 cm and $\varepsilon_{frozen\ ground}$ = 6-j). The snow parameters are selected to represent the typical cases in Finland. However, both snow and ground surface roughness characteristics represent the average values reported in the literature (Fung 1994, Shi and Dozier 1995, Kendra et al. 1998) and snow crystal size represents the effective snow crystal size (Kendra et al. 1998, Paper E).*

2.2 Backscattering from dry snow-covered terrain

Due to the fact that the dielectric contrast at the air-snow boundary is small for dry snow, the reflection coefficient is also quite small which means that the contribution

from the snow surface to the total backscattering coefficient is very small and can be neglected in most cases. Also the contributions from multiple reflections involving the upper and lower boundaries are much smaller than direct contributions. Because of the small dielectric contrast the roughness of the dry snow layer is not so important and the snow layer can be modeled as an inhomogeneous layer with a plane top boundary and a rough bottom boundary. The dry snow layer consists of air and randomly located ice particles of various sizes. Therefore the volume scattering in the snow layer is governed primarily by the size of the ice crystals compared to the wavelength. The ground contribution decreases as the snow depth (attenuation) increases *(Ulaby et al. 1986).*

Based on the observations, modeling and results reported in the literature the following conclusions can be drawn concerning the backscattering from dry snow at 5 GHz:

- the backscattering coefficient increases as a function of snow water equivalent due to the growing effect of volume scattering (the magnitude depends on the size of ice particles and used frequency) (see Figure 3) *(Ulaby et al. 1986, Shi et al. 1993, Paper E, Shi and Dozier 1999b),*
- the backscattering coefficient decreases with incresing incidence angle, due to the decreasing backscatter from the underlying ground (see Figure 3) *(Mätzler and Schanda 1984, Ulaby et al. 1986, Paper E),*
- the surface roughness of the dry snow layer has almost no contribution to the backscattering. Most of the backscattering comes from the snow layer and the snow-ground interface (see Figure 2) *(Ulaby et al. 1986, Shi et al. 1993, Paper E, Shi and Dozier 1999b).*

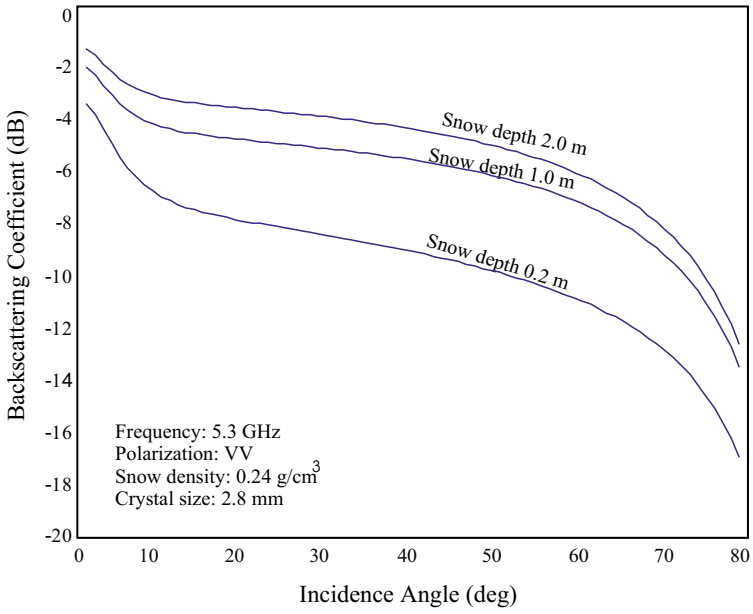

Figure 3. *Computed effect of snow depth to backscattering coefficient as a function of incidence angle (snow surface rms height (σ_s) = 0.4 cm, snow surface correlation length (l) = 5.0 cm, ground surface rms height (σ_g) = 1.2 cm and $\varepsilon_{frozen\ ground}$ = 6-j). The computation is based on the backscattering model introduced in Chapter 2.1.2.*

2.3 Backscattering from wet snow-covered terrain

While in the case of dry snow the roughness of the snow surface has an almost negligible effect on backscattering the effect is very strong in the case of wet snow. This effect is related to the change in the permittivity of snow. Due to the increase of permittivity the reflectivity of wet snow is higher than that of dry snow. Therefore, the surface roughness of wet snow is important and the snow-air interface has to be modeled as a rough surface in contrast to the dry snow case. As the dielectric loss factor of snow increases with increasing snow wetness *(Hallikainen et al. 1986)*, the absorption of wet snow layer becomes high and, consequently, the contribution from the ground decreases. Therefore, the increase of snow wetness causes a decrease in total backscattering as shown in Figure 4. In Figure 4 the backscattering coefficient in dB scale decreases quite linearly up to about 2 percent of volumetric wetness. The increase of incidence angle causes a general decrease in the absolute backscattering level but the behavior as a function of snow wetness is similar for incidence angles from 20 to 60 degrees *(Ulaby et al. 1986, Paper E).* In Figure 5 the diurnal behavior of the backscattering coefficient at various frequencies is plotted along with the snow wetness as a function of time.

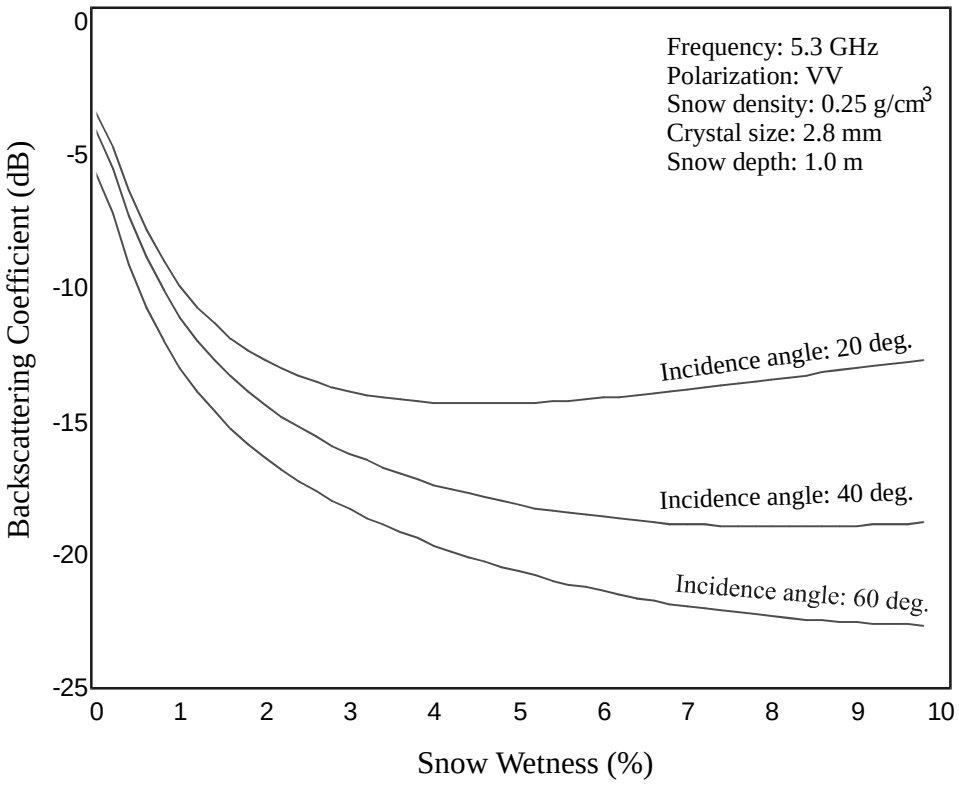

Figure 4. *The effect of snow volumetric wetness to the backscattering coefficient at various incidence angles (snow surface rms height (σ_s) = 0.4 cm, snow surface correlation length (l) = 5.0 cm, ground surface rms height (σ_g) = 1.2 cm and $\varepsilon_{frozen\ ground}$ = 6-j). The computation is based on the backscattering model introduced in Chapter 2.1.2.*

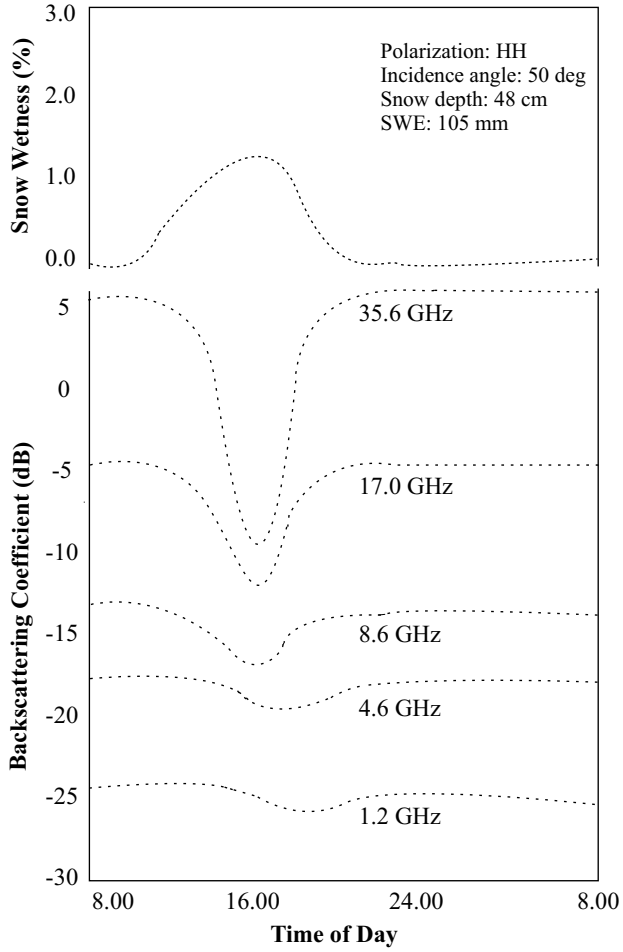

Figure 5. *Observed diurnal patterns of liquid water content, and backscattering coefficient at several microwave frequencies (Stiles et al. 1980).*

Based on the observations, modeling and results reported in the literature the following conclusions can be drawn concerning the backscattering from wet snow at 5 GHz:

- the level of backscatter from wet snow is generally lower than that from dry snow (depending on the surface roughness and incidence angle) due to the increase of absorption. The σ^o decreases almost linearly with increasing snow wetness (up to about 2 percent) as indicated by Figures 4 and 5 *(Stiles et al. 1980, Ulaby et al. 1986, Fung 1994, Paper E),*

- the difference between backscattering from dry snow and wet snow increases with increasing incidence angle when the snow surface layer is smooth (see Figure 3) *(Ulaby et al. 1986, Guneriussen et al. 1996, Paper E),* and

- the backscattering coefficient of wet snow does not depend on the snow water equivalent but it is highly dependent on the snow layer wetness and roughness of the snow cover because the major contribution of backscatter is caused by the air-snow interface *(Ulaby et al. 1986, Fung 1994, Shi and Dozier 1995, Paper E).*

2.4 Backscattering from forested terrain in snow-free and snow-covered conditions

2.4.1 General behavior of backscattering coefficient in forest

In the case of non-forested bare ground the backscattering coefficient generally increases with increasing soil moisture. The magnitude of increase is dependent on soil type but not so much on the used frequency. For small incidence angles ($\theta \leq 10^o$) the increase of surface roughness decreases the backscattering coefficient, whereas for larger incidence angles ($\theta > 15^o$) the effect is opposite *(Ulaby et al. 1986)*.

Due to the scattering and absorption by vegetation the contribution from the ground is smaller. At 1.2 GHz (L-band) most of the backscattering from vegetation comes from the trunks and big branches. At higher frequencies the main backscattering contribution comes from leaves and small branches. Increasing canopy moisture also increases the backscattering coefficient and, generally, after rain the total backscattering from forest is higher than before precipitation. Due to the volume scattering caused by canopy the effect of incidence angle for forested terrain is much smaller than for bare ground *(Ulaby et al. 1986)*.

2.4.2 Backscattering contribution from canopy and ground

The backscattering coefficient can be divided into four components in the case of forested terrain (see Figure 6). The backscattered signal measured by the radar is the sum of signal contributions from:

A) the crown layer,

B) ground,

C) trunk, and

D) trunk-ground reflections.

All these contributions are also affected by forest canopy transmissivity.

An example of the magnitude of the backscattering contributions at C-band is shown in Figure 7. This figure was obtained by simulating the backscattering contributions with the HUT boreal forest semi-empirical backscattering model *(Pulliainen 1994)*. The trunk-ground reflection is very small due to the Brewster angle effect; the vertically polarized wave does not reflect from the trunk but; rather, it totally penetrates the woody tissue *(Attema et al. 1978, Ulaby et al. 1982, Oh et. al. 1992, Pulliainen et al. 1994, Pulliainen et al. 1996b)*.

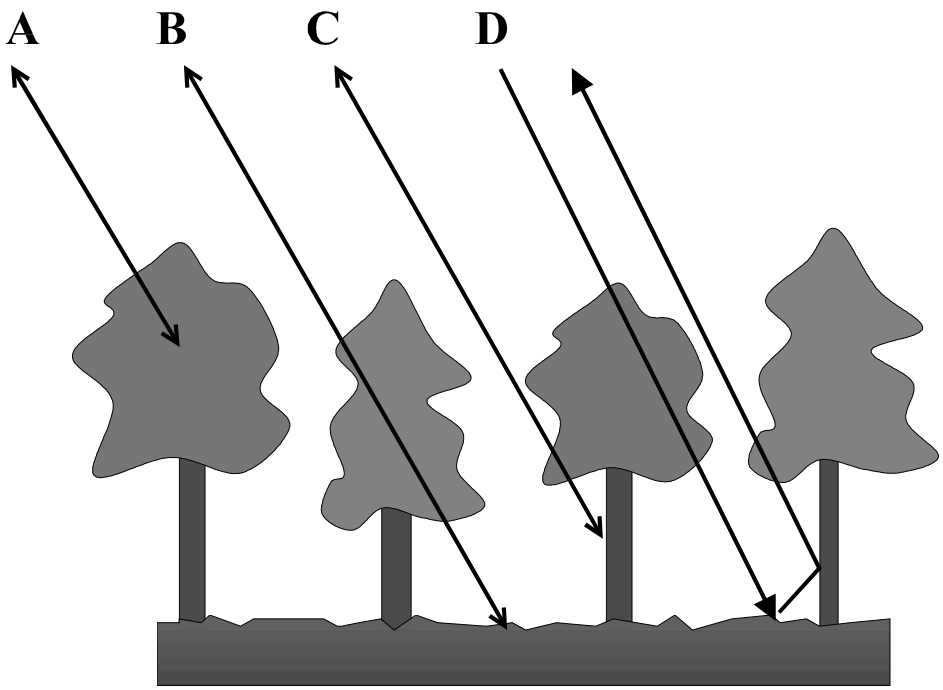

Figure 6. *Backscattering mechanisms of forest canopies. The total observed backscattering coefficient is the sum of contributions from (A) crown layer of the forest, (B) ground, (C) trunk and (D) trunk-ground reflections.*

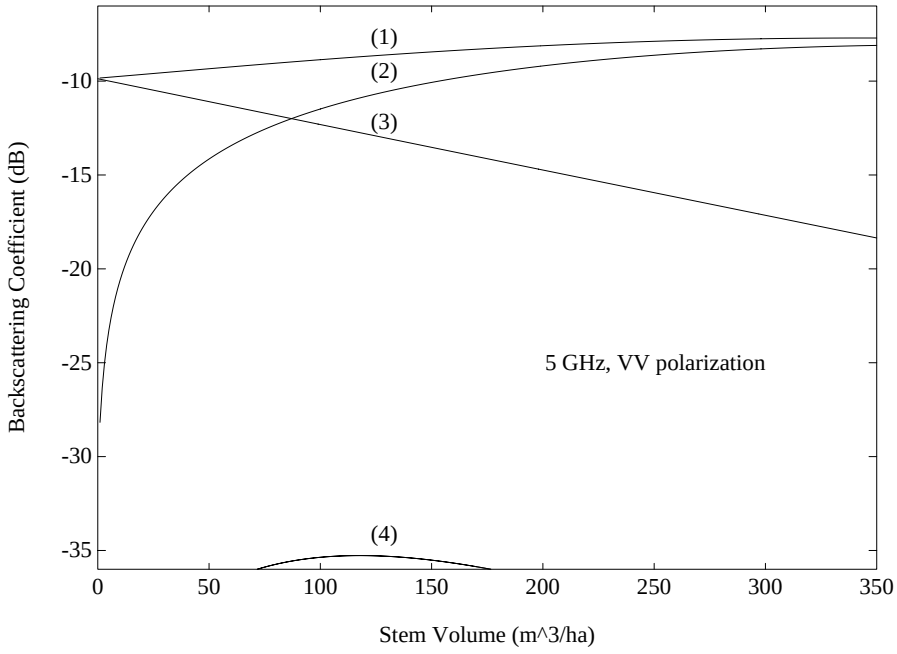

Figure 7. *Computed backscattering contributions at 5.3 GHz, VV polarization and 23^o incidence angle in wet snow conditions: (1) total backscattering coefficient, (2) canopy backscattering contribution, (3) soil backscattering contribution and (4) trunk-ground corner reflection (Pulliainen et al. 1994).*

2.5 Methods to retrieve snow information from backscattering signature

The capability of single-polarization and single-frequency SAR such as ERS SAR is limited in snow applications *(Koskinen et al. 1994, Piesbergen et al. 1995, Paper B, Guneriussen et al. 1997)*. A theoretical relation between the snow thermal resistance (which is a function of the thickness and density of snow) and backscattering coefficient has been reported previously, suggesting a possibility to estimate the snow water equivalent from the backscattering) *(Bernier and Fortin 1993)*. However, no experimental proof of this has been published. Although the ERS SAR system cannot differentiate dry snow and bare ground, it can discriminate wet snow from other snow/ground conditions *(Koskinen et al. 1994, Paper B)*. This has led to the development of a method that employs multi-temporal SAR images to monitor snow melt *(Paper B, Piesbergen et al. 1995, Paper D)*. Based on these results the fraction of snow-free ground in a SAR image can be estimated by comparing it with two other images, one acquired at the beginning of the melt period (wet snow) and the other acquired after the melt period (thawed snow-free ground) *(Paper B)*.

The following conclusions can be stated concerning active microwave remote sensing of snow by using a single-band and single-polarization (C-band, VV) radar and a small angle of incidence (23^{o}):

- in most cases wet snow can be discriminated from snow-free ground *(Koskinen et al. 1994, Paper B, Paper D, Paper E)*. The discrimination accuracy is highly dependant on the snow wetness (see Figures 4 and 9) *(Paper E)*,

- dry snow cannot be discriminated from snow-free ground (see Figure 9) *(Koskinen et al. 1994, Paper B)*,

- the backscattering coefficient depends on the snow layer wetness, not so much on the thickness, or density of the snow layer (see Figures 3 and 4). However, for shallow dry snow layer the ground contribution dominates and the backscattering is lower than for thicker snow layers as shown in Figure 3 *(Stiles and Ulaby 1980, Paper E)*,

- the level of backscattering from wet snow depends on the surface roughness, because most of the backscattering is due to the air/snow interface. Rougher surfaces cause higher backscattering while often the wet snow surface is smooth and the backscattering is low due to the mirror-like reflection on the surface of the snow layer *(Mäzler and Schanda 1983, Stiles and Ulaby 1980, Paper E)*,

- the backscattering level for snow-free ground is dependent on the soil and canopy moisture *(Pulliainen et al. 1994, Pulliainen et al. 1996b*). The backscattering from dry ground is low and it increases as the soil and canopy moisture increase,

- the backscattering coefficient has a positive correlation with forest stem volume in the case of wet snow or dry soil and canopy. However, for moist soil and canopy the correlation is negative *(Paper C, Paper E),*

- by employing theoretical and semi-empirical models the backscattering coefficient for forested terrain can be divided into contributions from the canopy and forest floor and, therefore, information on the snow layer can be retrieved even in the presence of forest canopies *(Paper C, Paper E),*

- in mountainous terrain, geocoded SAR data is required; correction due to the local incidence angle will improve the contrast between wet snow and bare ground (see Figure 4) *(Guneriussen et al. 1997),*

- progress in snow melt can be monitored by comparing SAR images acquired during the melt season with two reference images (SAR images acquired before and after the melt season). Snow melt maps indicating the fractions of bare ground and melting (wet) snow can be derived from the comparison *(Paper B, Paper D).* However, forest canopy moisture variations and thawing cause some uncertainty to the estimation *(Paper C, Paper E).*

Multi-parameter SAR provides information on various layers of the snow-covered terrain. High frequencies (X band) respond to small changes in the snow wetness and cause the backscattering to be dominated by the snow-air interface, while low frequencies penetrate the snow layer and most of the backscattering is due to increased volume scattering and the snow-ground interface *(Stiles and Ulaby 1980).*

Shi and Dozier have studied the relation between polarimetric C-band signatures versus snow wetness *(Shi and Dozier 1995)* and L-, C- and X-band signatures versus snow water equivalent *(Shi et al. 1993).* The studies were conducted using SIR-C/X data from the Mammoth Mountains in California. They employed the ratio between like polarizations ($\sigma^0_{vv}/\sigma^0_{hh}$) to retrieve snow wetness, while for snow water equivalent retrieval they used multiple frequencies. However, these results included few samples and, therefore, it is very difficult to verify the retrieval accuracy for these methods.

By using a combination of multiple bands and polarizations

- dry snow can be discriminated from bare ground using X-band data. The best classification results of different snow/ground categories (dry snow, wet snow and frozen ground) are obtained using a combination of C- and X-band *(Jääskeläinen 1993),*

- a rough estimate for snow wetness (ratio between C-band VV and HH polarizations) and snow water equivalent (combination of L, C and X band polarimetric backscattering signatures) can be derived *(Shi et al. 1993, Shi and Dozier 1995)* and

- information on the structure (particle size, density and layers) of snow can be obtained. Lower frequencies (L- and C- band) penetrate the snow layer, while the backscattering at higher frequencies (X-band) is due to the air-snow boundary. Lower frequencies are less sensitive to changes in the snow layer (density, depth, wetness and layering), while higher frequencies react to smaller anomalies in the snow layer. L-band can be used to estimate snow density and subsurface properties (roughness) due to small volume scattering and extinction in snow layer *(Shi and Dozier 1999a)*, while X-band can be employed to retrieve an estimate to the particle size *(Shi and Dozier 1999b)*.

Based on recent radar studies only snow extent mapping during the snow melt season seems feasible, because all SAR satellites employ single-frequency and single-polarization radar. However, an operational application would also need a regular revisit time (once a week) and fast processing services (few hours from the satellite pass). In the near future the launch of ENVISAT (C-band, VV, VH and HH -polarization) and possibly USSAR (former LightSAR, L-band VV- and HH-polarization and possible X-band) will provide more multi-channel SAR data. However, the operational hydrological application would need multiple frequencies in the same satellite radar in order to obtain simultaneously information on the air-snow interface, the snow layer and on the snow-ground interface.

3. Results and Discussion

3.1 Seasonal radar response to land-use categories

Backscattering is strongly affected by the soil and canopy moisture and surface roughness. The potential of microwave radar in land-use classification is related to the possibility to discriminate land-use classes, which differ from each other with respect to these characteristics *(Ulaby et al. 1986, Guyenne 1995, Guyenne and Bernards 1995).* As several parameters contribute to the level of backscattering it is difficult to discriminate land-use classes using a single SAR image. However, by studying the seasonal variations of backscattering some land-use classes can be discriminated *(Paper A).* In Finland seasonal snow cover adds an extra feature to the seasonal behavior. As explained in Chapter 2 dry snow slightly attenuates the radar signal and causes volume scattering at C-band, but wet snow cover masks out short vegetation and small soil roughness and, therefore, increases correlation with the forest stem volume *(Pulliainen et al. 1996b, Paper A, Paper B).* For snow-free terrain the correlation between the backscattering coefficient and stem volume may be negative, while in the case of wet snow it is positive as shown in Figure 8.

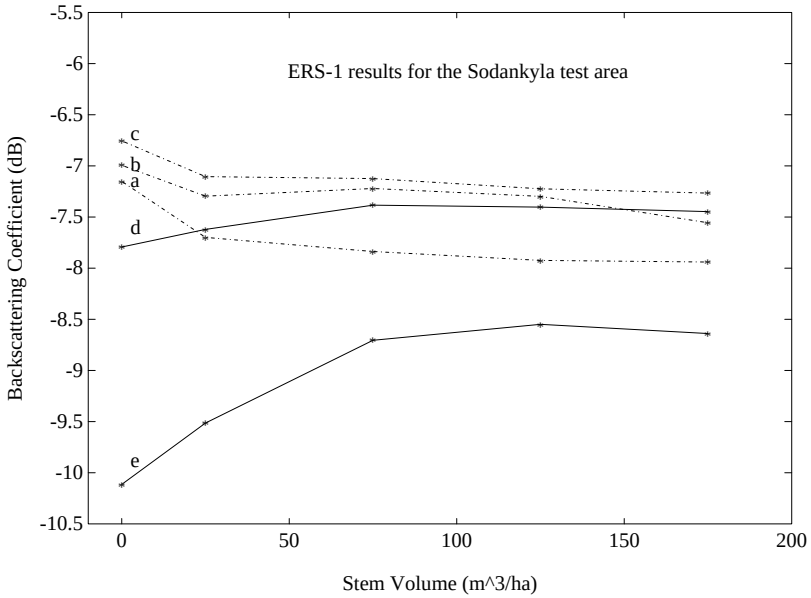

Figure 8. *ERS-1 SAR results for the Sodankylä test area under summer and winter conditions. Curves (a)-(c) show the summer time responses and the curves e) and d) show the winter time responses. (a) 24 June 1992 (no snow), (c) 29 July 1992 (no snow), (e) 1 May 1992 (wet snow), (b) 18 September 1992 (no snow) and (d) 20 January 1993 (dry snow). The results are presented for clear-cut areas (0 m^3/ha) and four stem volume classes: 0-50 m^3/ha, 50-100 m^3/ha, 100-150 m^3/ha and 150-200 m^3/ha (Paper A).*

By comparing the first three principal components of 16 SAR images and a land-use map from the Sodankylä test site (40 km by 40 km) significant correspondences were noticed which suggests the possibility to use multi-temporal ERS-1 SAR images for land-use classification. Especially moist land-use classes (bogs and mires) were visible *(Paper A).* Based on visual observations and the analysis conducted using the boreal forest semi-empirical backscattering model six land-use classes were chosen to represent the whole test area *(Paper A).* These classes are shown in Table 2.

The results obtained by using supervised classification and the first three principal components are summarized in a confusion matrix in Table 2. The total classification accuracy was 43 % for the six classes employed. The best results were obtained for the classification of (1) land vs. water, and (2) mineral soil vs. peat land (mires and bogs). The results suggest that water, peat land and mineral soil areas can be discriminated. The accuracy of stem volume classification was below the average classification accuracy. An obvious reason to this is that there were actually three different categories of vegetation (mire and two forest stem volume classes) in the classification. If the two stem volume classes had been combined to a single class (forest on mineral soil), accuracy would obviously have been higher. The most difficult task for the algorithm was to identify open areas. This is due to the large variability (clear-cut, field, gravel) within this class *(Paper A).*

Table 2. *Confusion matrix for supervised land use classification. The classification was made by employing multi-temporal ERS-1 SAR data from Sodankylä test site during years 1991-1993 (Paper A). The rows present the results of classification in percent. The classes on the columns are from the reference land-use map, which is based on classification made using optical (Landsat and Spot) images. The reference map has a reported accuracy of 65 to 100 % depending on the land-use class (Paavilainen et al. 1992)*

Class	**Water**	**Forest below 100m^3/ha**	**Forest above 100m^3/ha**	**Open area**	**Open bog**	**Mire**	**Classification accuracy %**
Water	**82**	1	-	-	2	-	82
Forest below 100m^3/ha	0	**42**	36	29	8	21	42
Forest above 100m^3/ha	0	23	**38**	11	3	9	38
Open area	15	7	7	**18**	3	4	18
Open bog	3	6	4	7	**54**	10	54
Mire	0	21	15	35	30	**56**	56
Total of samples	51207	1103531	257755	240604	283462	180552	**43**

3.2 Mapping of snow/ground condition and snow extent

The seasonal SAR data of 21 images acquired during years 1991 to 1993 was divided into four categories (wet snow, dry snow, thawed snow-free ground, frozen snow-free ground) by using weather information. The mean backscattering coefficients of SAR data was calculated for each land-use class in different seasonal conditions. Figure 9 shows that the mean backscattering values for wet snow conditions are clearly different from those for other categories. This suggests that the potential of ERS-1 SAR in discriminating snow from soil categories is limited to wet snow detection *(Paper B)*. The difference between the mean value of the backscattering coefficients for wet snow and the other categories is about 3 dB for open areas. The difference decreases with increasing biomass in the test site shown in Figure 9. In case the ground is covered by wet snow layer the backscattering coefficient increases as a function of stem volume. The backscattering portion caused by the snow layer decreases as the stem volume increases, since the absorption and scattering by the forest canopy increases. Forest canopy causes higher backscattering than wet snow and as a result the total backscattering coefficient increases as shown in Figure 8 (curve e).

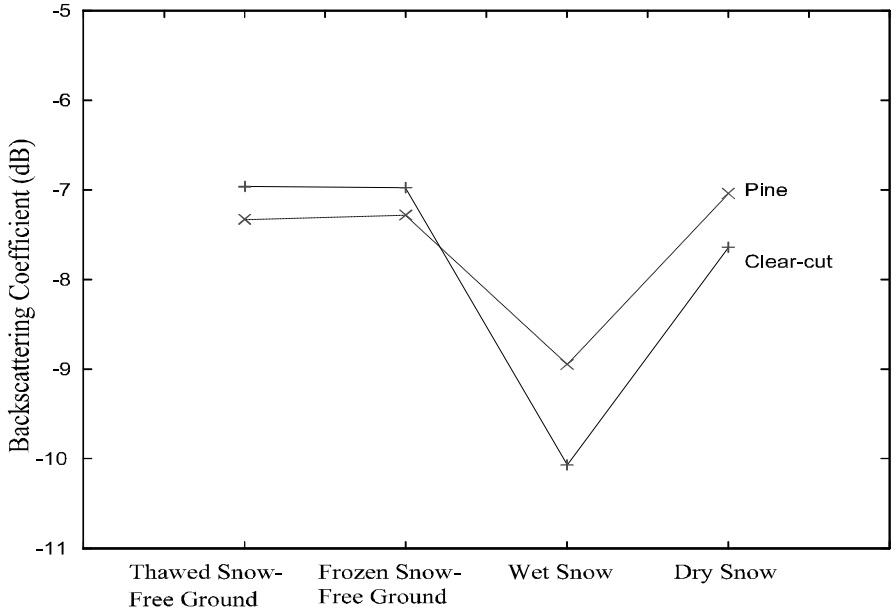

Figure 9. *ERS-1 SAR derived average backscattering coefficients for clear-cut and forested areas (stem volume 50-100 m^3/ha) in different snow conditions in Sodankylä test site. The data was collected during years 1991 to 1993 (Paper B).*

The fact that wet snow can be discriminated from snow-free ground suggested the possibility to develop a method for mapping the snow extent during the snow melt period. The algorithm developed in Paper B observes the pixel-wise backscattering coefficient of an image acquired during the snow melt period relative to those of the two images acquired at the beginning and after the melt period *(Paper B).* The idea of the algorithm is shown in Figure 10.

The functionality of the algorithm was tested by producing snow melt maps for the River Kemi drainage area. These maps were compared with daily visual observations of the snow/ground condition at each weather station. As indicated in Table 3, the SAR-derived snow extent percentage behaves logically when compared with observations at the weather stations, i.e. when the weather station observation changes from the total snow cover towards snow-free condition also the SAR-derived snow extent percentage decreases. However, the SAR-derived snow extent percentage decreases within the same weather station observation class during the three sample dates. The main reason for this behavior is that all ground observations are made only near the weather station and so the spatial coverage is poor compared to SAR-derived estimates *(Paper D).*

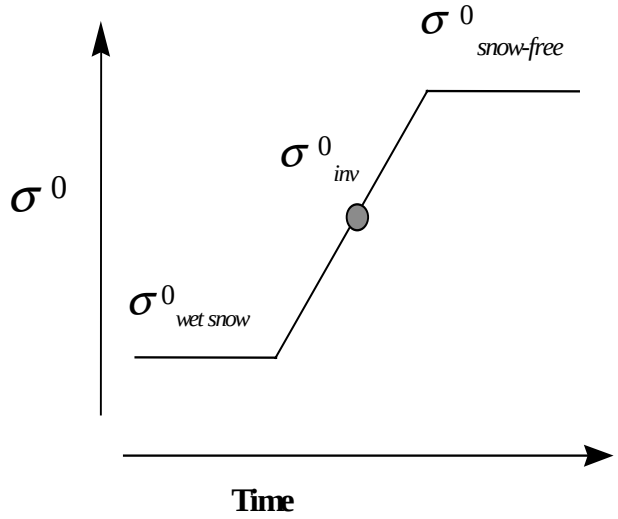

Figure 10. *Sketch of the evolution of backscattering coefficient (σ^0) as a function of time during snow the melt period. The $\sigma^0_{wet\ snow}$ value is the backscattering coefficient at the time when the whole pixel is covered by wet snow, the σ^0_{inv} value is related to the investigated situation and the $\sigma^0_{snow\text{-}free}$ value is the backscattering coefficient at the time when all snow has melted within the pixel.*

Table 3. *Comparison of SAR-derived snow extent and ground data collected from the weather stations. The SAR derived value represents the mean and standard deviation of pixel-wise snow extent estimates within the weather station observation area (Paper D).*

Weather station based observation for snow extent (%)	**SAR-derived estimate for snow extent (%)**		
	May 25, 1997	**May 28, 1997**	**June 4, 1997**
Totally covered by snow (100%)	-	-	-
More than half of the area covered by snow (>50%)	76 ± 20	73 ± 13	-
Less than half of the area covered by snow (<50%)	68 ± 23	48 ± 27	23 ± 10
Snow exists only in forest	49 ± 20	31 ± 18	14 ± 13
Snow-free (0%)	-	29 ± 15	0

3.3 Application of the HUT boreal forest backscattering model for snow monitoring

The boreal forest backscattering model *(Pulliainen 1994)* was used in Paper A and Paper B to simulate the effect of ground and forest canopy moisture to the backscattering coefficient. The model provides important information on the backscattering behavior in varying seasonal conditions as a function of stem volume. In Paper C that is based on the simultaneous measurements of HUTSCAT ranging scatterometer and ERS-1 SAR, the model was used to estimate the magnitude of various backscattering mechanisms in spaceborne SAR observations. The model simulations were conducted in various seasonal conditions in order to determine how the backscattering contributions from the forest canopy and forest floor, as well as the total backscatter, change, and to determine the instrument response to the biomass. By employing the ranging capability of HUTSCAT scatterometer the measurement spectrum from forest area can be divided into (a) backscattering portion caused by top of the canopy and (b) portion caused by ground and multiple scattering. Statistical analysis of HUTSCAT and ERS-1 SAR measurements verifies the similar behavior of these data sets and, therefore, justifies the use of boreal forest backscattering model in the analysis of various scattering contributions of ERS-1 SAR measurements. Figure 11 shows the ERS-1 SAR backscattering coefficient divided into ground and canopy contributions in wet snow conditions.

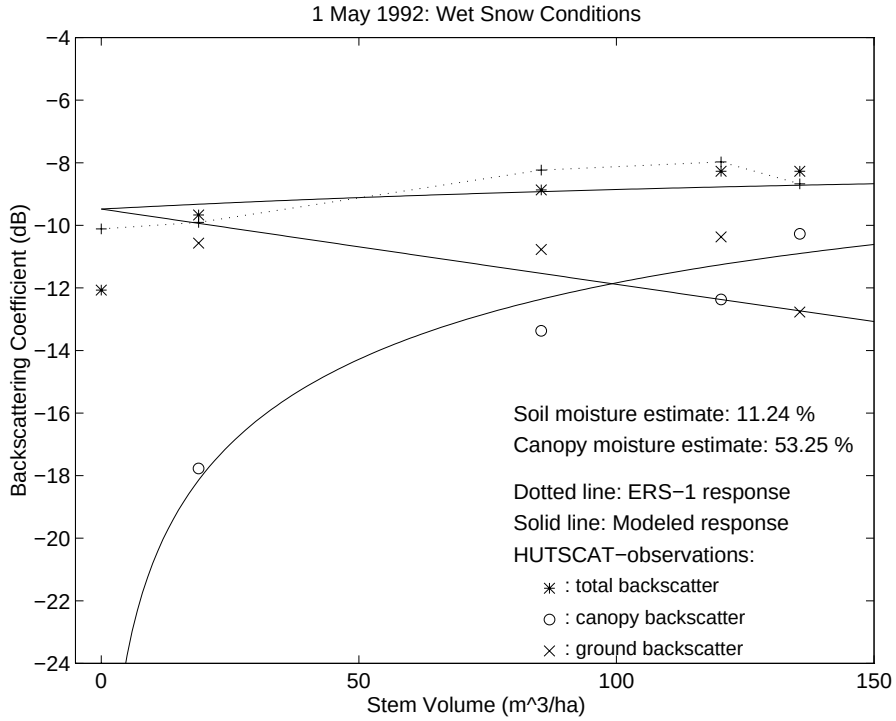

Figure 11. *Observed behavior of ERS-1 SAR and HUTSCAT-derived total backscattering coefficients and modeled backscattering contributions obtained by fitting the semi-empirical backscattering model into HUTSCAT observations in wet snow conditions. The estimated effective soil moisture value (11.24%) corresponds to the dry/frozen ground, which has similar backscattering magnitude as wet snow (Paper C).*

The results indicate that the use of the semi-empirical model and HUTSCAT data allow quantitative clarification of how various scattering mechanisms affect ERS-1 SAR results under different seasonal conditions and for different types of forest canopies. The novel features introduced in Paper C include the possibility to extract the backscattering contribution from the forest canopy and analyze the forest ground layer backscattering contribution. Therefore, by using the model together with ERS SAR measurements we can better analyze the backscattering from the snow layer in forested area by extracting the backscattering caused by the forest canopy and thus monitor more closely the behavior of snow layer in forested area as verified in Paper E.

3.4 Effect of various snow parameters to the accuracy of HUT snow melt algorithm

The HUT snow melt algorithm has been developed using ERS-1 SAR measurements. The main principle of the HUT snow melt algorithm is that the fraction of snow cover in every pixel is estimated by comparing a SAR image acquired during the snow melt period with the reference images acquired at the beginning of the snow melt period (the whole area is covered by wet snow) and after the snow melt period (the whole area is snow-free wet ground). By applying the backscattering model presented in Paper E and discussed in Chapter 2.1.2 we can investigate the effect of various snow parameters to the total backscattering coefficient of snow-covered terrain. This information can be used to compare the accuracy characteristics of the snow melt algorithm. Figure 12 shows the modeled ratio of σ^0 for wet ground to σ^0 for wet snow with various combinations of physical snow characteristics. In the simulation of Figure 12 the following ranges of parameter values were used:

- snow depth: 20 to 200 cm,
- snow density: 0.2 to 0.5 g/cm^3,
- snow crystal size: 2.0 to 4.0 mm,
- snow surface roughness: rms 0.4 cm , correlation length 5.0 cm
- snow-free ground moisture: 25 to 30 %,
- ground surface roughness: rms 1.2 cm,
- radar: C-band, VV-polarization and incidence angle 23 degrees.

The variation ranges are selected to represent the typical cases in Finland. However, both snow and ground surface roughness characteristics represent the average values reported in the literature *(Fung 1994, Shi and Dozier 1995, Kendra et al. 1998)* and snow crystal size represents the effective snow crystal size *(Kendra et al. 1998, Paper E).* The results are presented as a function of snow wetness. The vertical bars indicate the variation caused by the above parameters within their respective ranges.

In Figure 12 the results of the simulations of the HUT snow melt algorithm show that the standard deviation of backscattering difference decreases as the snow wetness increases. Most of the variation in the case of low snow wetness is due to the variation of volume scattering in the snow layer. For thin snow layers (0.5 m) the effect of ground scattering dominates and, therefore, the total backscattering is lower than that for thicker snow layers where the volume effect dominates. The smallest variation is obtained when snow wetness is above 2 %. In this case the standard deviation of the snow melt algorithm is less than 2 dB (the mean difference varies from 6.5 to 7.4 dB). In principle the level of snow-free ground backscattering in the HUT snow melt algorithm also depends on the surface roughness, but because the comparison is always done pixel-wise this effect can be eliminated *(Paper E).*

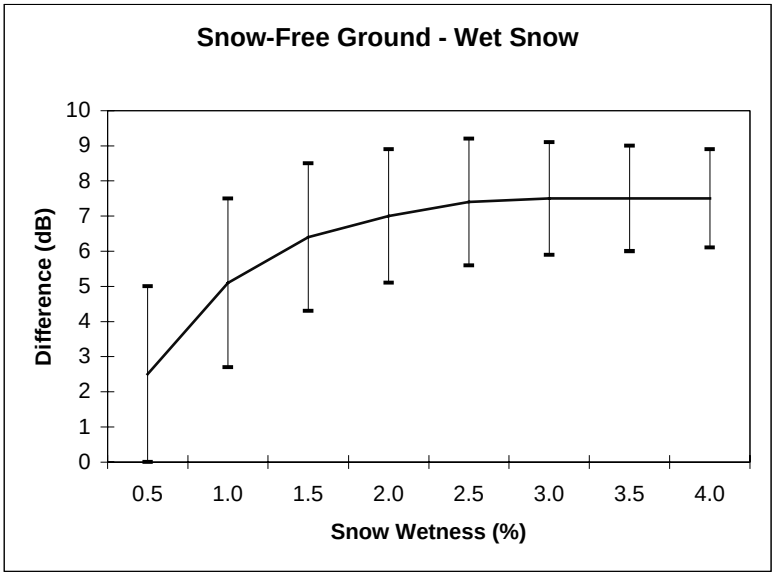

Figure 12. *The behavior of backscattering coefficient difference between wet snow and snow-free ground as a function of snow wetness. The calculation is based on various snow depths (20-200 cm), snow densities (0.2-0.5 g/cm^3) and snow crystal sizes (2.0-4.0 mm). The vertical bars indicate the standard deviation of the mean backscattering differences (Paper E).*

3.5 Combined use of optical and SAR data

Optical satellite data is used operationally in snow extent monitoring *(Solberg 1997);* however, the availability of optical data is very limited due to the clouds and weather conditions especially in spring. Therefore, the need for microwave data is obvious. The results in Paper D show that the surface reflectance obtained from NOAA AVHRR observations agrees with the snow cover percentage derived from SAR data. The comparison was carried out for a single SAR and AVHRR image acquired at the begining of June 1997. The correlation of AVHRR and SAR results were analyzed for various landcover / vegetation classes. In Figure 13 AVHRR reflectances (visible channel) are plotted against SAR-derived proportions of snow-free ground. The correlation between AVHRR-derived reflectance and SAR-derived proportion of snow-free ground for non-forested terrain in mineral soil is good (R = 0.82).

However, for forested terrain the correlation between NOAA and SAR observation decreases (R = 0.63). This is mainly because the visible and near infrared waves cannot penetrate the forest canopy, while microwave frequencies provide information also on the forest ground layer. The worst correlation (R = 0.37) was obtained for a class, which was a combination of mire and sparse forest on mineral land. The poor correlation is most likely due to the different properties of these classes. Especially the SAR-derived results can be affected by the large water content in mires after the snow melt; some of the mires can have ponds which strongly effect the backscattering coefficient measured by SAR and, therefore, lead to poor estimation of snow cover percentage.

The good correlation between SAR- and NOAA-derived values will benefit the operational snow cover mapping methods; when optical data is not available it can be replaced with SAR data.

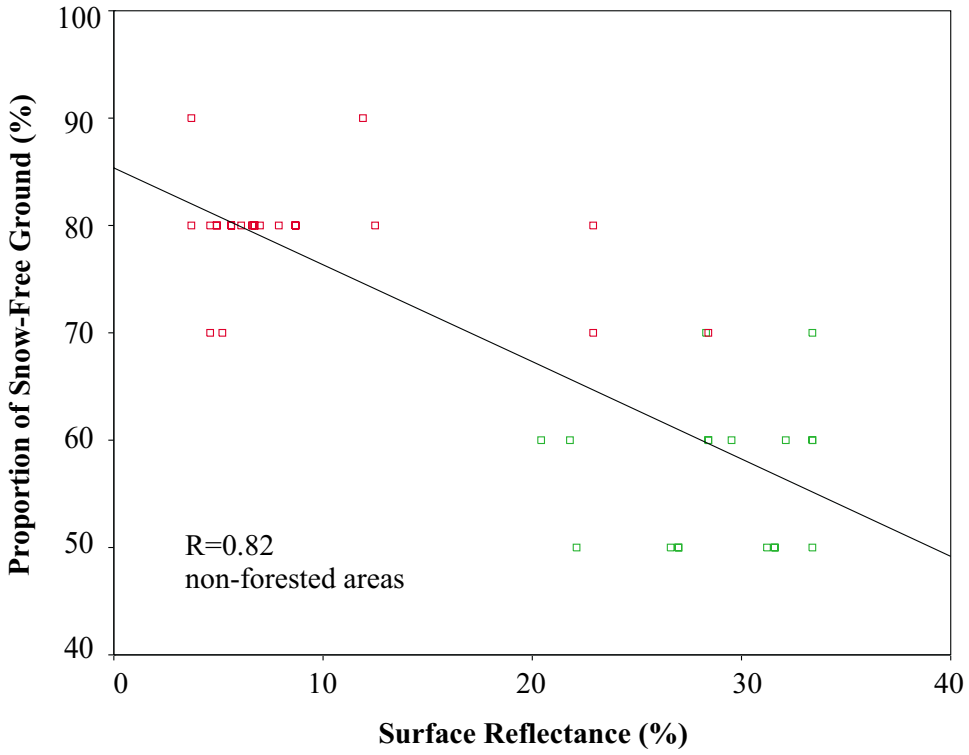

Figure 13. *SAR-derived proportion of snow-free ground against AVHRR visible frequency channel-derived reflectances in non-forested areas (Paper D).*

4. Summary of Appended Papers

All papers concentrate in remote sensing of snow and the emphasis in all papers is in active microwave sensors.

In Paper A seasonal radar response to land-use is observed with ERS-1 SAR. In the study a total of 16 SAR images in various seasonal conditions are employed. In order to compress the data set and decrease the effect of speckle principal component analysis is used. Both supervised and unsupervised classification experiments are done using the first three principal components. The results are compared with a land-use map, which is produced by National Land Survey of Finland using optical satellite data and ground surveys. Both supervised and unsupervised land-use classification conducted using radar data show results similar to the classification based on optical data.

Paper B describes the general backscattering behavior of different snow types (dry and wet snow) and snow-free ground in northern Finland. Based on the observations a novel pixel-wise snow cover classifier is developed. As a result of the classification a map showing the proportion of snow-covered ground versus snow-free ground is obtained. The results have been compared with model simulations and visual interpretation based on airborne video.

In Paper C a comparison of airborne ranging scatterometer and spaceborne SAR data is presented. The emphasis is on combined use of airborne and spaceborne radar in boreal forest and snow monitoring. The measurements are compared in five different seasonal conditions and for various land-use categories. Based on statistical analysis the behavior of airborne ranging scatterometer and spaceborne SAR data is similar in various seasonal conditions and for various land-use categories. By applying the HUT boreal forest backscattering model and the statistical comparison of HUTSCAT and ERS-1 SAR the backscattering coefficient of ERS-1 SAR in forest areas can be divided into two contributions: (1) contribution from forest canopy and (2) contribution from ground. This information helps us to monitor the backscattering behavior of underlying soil/snow for forested terrain.

Paper D can be regarded as a follow-up study for Paper B. In this study the classification algorithm developed in Paper B is further verified with a larger SAR data set. The SAR-derived results are also compared with optical NOAA AVHRR-derived reflectances and operationally used *in situ* surveys. The results show that the algorithm developed in Paper B works well and the snow melt maps correlate with the optical data set. According to these results the remotely sensed data would benefit the operational snow melt forecasts by providing a larger spatial coverage than ground surveys made on snow courses. Also more frequent information can be obtained by using remotely sensed data instead of *in situ* surveys which are done only once a month.

Paper E presents a backscattering model for snow. By applying this model the effect of various snow properties to the backscattering at C-band, VV-polarization is

simulated. Based on the results obtained in Paper C the snow model is combined with the HUT boreal forest backscattering model so that it is possible to analyze snow cover also in forested areas. The model is verified using HUTSCAT- and ERS-measurements conducted in Sodankylä. The model is used to theoretically analyze the effect of various snow parameters to the snow melt algorithm presented in Papers B and D. Based on the model simulations theoretical accuracy values are derived for the snow melt algorithm.

5. References

E. Attema and F. Ulaby, "Vegetation Modeled as Water Cloud", *Radio Science*, Vol. 13, pp. 357-364, 1978.

M. Bernier and J. Fortin, “Potential of ERS-1 SAR Data to Snow Cover Monitoring”, *Digest IEEE International Symposium on Geoscience and Remote Sensing (IGARSS’93)*, Houston, Texas, USA, pp.1664-1666, 1993.

A. Denoth, “Snow Dielectric Measurements”, Adv. Space Res., Vol. 9, No. 1, pp., 233-243, 1989.

A. Fung, “Microwave Scattering and Emission Models and Their Applications”, *Artech House*, 573 p., 1994.

T. Guneriussen, H. Johnsen and K. Sand, “DEM Corrected ERS-1 SAR Data for Snow Monitoring”, *Int. Journal of Remote Sensing*, Vol. 17, No. 1, 1996.

T. Guyenne and F. Bernards (editors),“Land and Sea ERS-1 Applications”, *ESA, ESA BR-109*, Noordwijk, 1995.

T. Guyenne (editor), “Scientific Achievements of ERS-1”, *ESA SP-1176/I, ISBN 92-9092-141-2*, ESA-ESTEC, Noordwijk, 162 p., 1995.

M. Hallikainen, F. Ulaby and M. Abdelrazik, “Dielectric Properties of Snow in the 3-37 GHz Range”, *IEEE Trans. Antennas and Propagation*, Vol. 34, No. 11, pp. 1329-1340, 1986.

M. Hallikainen, F. Ulaby and T. Van Deventer, "Extinction Behavior of Dry Snow in the 18- to 90- GHz Range", *IEEE Trans. Geoscience and Remote Sensing*, Vol. 25, No. 6, pp. 737-745, 1987.

M. Hallikainen and P. Jolma, “Comparison of Algorithms for Retrieval of Snow Water Equivalent from Nimbus-7 SSMR Data in Finland”, *IEEE Trans. on Geoscience and Remote Sensing*, Vol. 30, No. 1, pp. 124-131, 1992.

V. Jääskeläinen, “Remote Sensing of Snow by Microwave Radar”, *Licentiate of Science in Technology Thesis, Laboratory of Space Technology, Helsinki University of Technology*, Espoo, 110 p. 1993.

J. Kendra, K. Sarabandi and F. Ulaby, "Radar Measurements of Snow: Experiments and Analysis", *IEEE Trans. Geoscience and Remote Sensing*, Vol. 36, No. 3, pp. 864-879, 1998.

J. Koskinen, L. Kurvonen, V. Jääskeläinen and M. Hallikainen, "Capability of Radar and Microwave Radiometer to Classify Snow Types in Forested Areas", *Digest IEEE International Symposium on Geoscience and Remote Sensing (IGARSS’94)*, Pasadena, USA, pp. 1283-1286, 1994.

R. Kuittinen, “Remote Sensing for Hydrology Progress and Prospects, *WMO Operational Hydrology report*, No. 36, WMO-No. 773, Geneva, Switzerland, 1992.

C. Mätzler and E. Schanda, “Snow Mapping with Active Microwave Sensors”, *International Journal of Remote Sensing*, Vol. 15, No. 2, pp. 409-422, 1983.

C. Mäzler, “Applications of the Interaction of Microwaves with the Natural Snow Cover”, *Remote Sensing Reviews*, Vol. 2, pp. 259-387, 1987.

C. Mätzler, “Passive Microwave Signatures of Landscapes in Winter”, *Meteorology and Atmospheric Physics*, Vol. 54, pp. 241-260, 1994.

C. Mäzler, “Microwave Permittivity of Dry Snow”, *IEEE Trans. Geoscience and Remote Sensing*, Vol. 34, No. 2, pp. 573-581, 1996.

T. Nagler and H. Rott, “SAR Tools for Snowmelt Modeling in the Project HydAlp”, *Digest IEEE International Symposium on Geoscience and Remote Sensing (IGARSS’98)*, Seattle, USA, 1998.

Y. Oh, K. Sarabandi and F. Ulaby, "An Empirical Model and Inversion Technique for Radar Scattering from Bare Soil Surfaces", *IEEE Trans. Geoscience and Remote Sensing*, Vol. 30, pp. 370-381, 1992.

J. Paavilainen, T. Siltala and A. Vertanen, "Digital Land-use Map, Product Specification", *National Land Survey, Department of Remote Sensing*, 1 p. 1992.

J. Piesbergen, F. Holecz, F. and H. Haefner, “Snow Cover Monitoring Using Multitemporal ERS-1 SAR Data”, *Digest IEEE International Symposium on Geoscience and Remote Sensing (IGARSS’95)*, Florence, Italy, pp. 1750-1752, 1995.

J. Perälä and M. Reuna, “The Areal and Time Variability of Snow Water Equivalent in Finland”, *Publication of the Water and Environment Administration*, series A 56, 257 p., 1990.

J. Pulliainen, "Investigation on the Backscattering Properties of Finnish Boreal Forests at C- and X-Band: a Semi-empirical Modeling Approach", *Doctor of Science in Technology Thesis, Report 19, Laboratory of Space Technology, Helsinki University of Technology*, Espoo, 119 p., 1994.

J. Pulliainen, K. Heiska, J. Hyyppä and M. Hallikainen, "Backscattering Properties of Boreal Forests at C- and X-Band", *IEEE Trans. Geoscience and Remote Sensing*, Vol. 32, No. 5, pp. 1041-1050, 1994.

J. Pulliainen , J. Grandell, M. Hallikainen, M. Virtanen, N. Walker, S. Metsämäki, J. Ikonen, Y. Sucksdorf and T. Manninen, “Scatterometer and Radiometer Land Applications”, Final Report, *ESRIN Contract No: 11122/94/I-HE(SC)*, 255 p., 1996a.

J. Pulliainen, P. Mikkelä, M. Hallikainen and J-P. Ikonen, "Seasonal Dynamics of C-Band Backscatter of Boreal Forests with Application to Biomass and Soil Moisture Estimation", *IEEE Trans. Geoscience and Remote Sensing*, Vol. 34, No. 3, pp. 758-770, 1996b.

A. Rango, "Progress of Snow Hydrology Remote Sensing Research", *IEEE Trans. on Geoscience and Remote Sensing*, Vol. 24, No. 7, pp. 47-53, 1986.

H. Rott, "The Analysis of Backscattering Properties from SAR Data of Mountain Region", *IEEE Journal of Oceanic Engineering*, Vol. 9, No. 5, pp. 347-355, 1984.

J. Shi, J. Dozier and H. Rott, "Deriving Snow Water Equivalence Using C-band Polarimetric SAR" *Digest IEEE International Symposium on Geoscience and Remote Sensing (IGARSS'93)*, Tokyo, Japan, pp. 1038-1041, 1993.

J. Shi and J. Dozier, "Inferring Snow Wetness Using C-band Data from SIR-C's Polarimetric Synthetic Aperture Radar" *IEEE Trans. Geoscience and Remote Sensing*, Vol. 33, No. 4, pp. 905-914, 1995.

J. Shi and J. Dozier, "Estimation of Snow Water Equivalence Using SIR-C/X-SAR – Part I: Inferring Dry Snow Density and Subsurface Properties" *IEEE Trans. Geoscience and Remote Sensing*, Submitted, 1999a.

J. Shi and J. Dozier, "Estimation of Snow Water Equivalence Using SIR-C/X-SAR – Part II: Inferring Snow Depth and Particle Size" *IEEE Trans. Geoscience and Remote Sensing*, Submitted, 1999b.

R. Solberg and T. Andersen, "An Automatic System for Operational Snow-Cover Monitoring in the Norwegian Mountain Regions", *Digest IEEE International Symposium on Geoscience and Remote Sensing (IGARSS'94)*, Pasadena, USA, pp. 1038-1041, 1994.

R. Solberg, D. Hiltbrunner, J. Koskinen, T. Gunneriussen, K. Rautiainen and M. Hallikainen, "Snow Algorithms and Products", Norwegian Computing Center, *Report 924*, Oslo, Norway, 112 p., 1997.

W. Stiles and F. Ulaby, "The Active and Passive Microwave Response to Snow Parameters: Part I - Wetness", *Journal of Geophysical Research*, No. 85, pp. 1037-1044, 1980.

L. Tsang, J. Kong and R. Shin, "Theory of Microwave Remote Sensing", *John Wiley & Sons*, 603 p., 1985.

F. Ulaby and W. Stiles, "Microwave Response of Snow", *Advanced Space Research*, No. 1, pp. 131-149, 1981a.

F. Ulaby, R. Moore and A. Fung, "Microwave Remote Sensing, Active and Passive", Volume I. *Reading, Addison Wesley*, 456 p. 1981b.

F. Ulaby, R. Moore and A. Fung, "Microwave Remote Sensing, Active and Passive", Volume II. *Reading, Addison Wesley*, 609 p. 1982.

F. Ulaby, R. Moore and A. Fung, "Microwave Remote Sensing, Active and Passive", *Volume III. Artech House*, 1100 p. 1986.

H. Wang, J. Pulliainen and M. Hallikainen, “Extinction Behavior of Dry Snow at Microwave Range up to 90 GHz by Using Strong Fluctuation Theory”, *Progress in Electromagnetic Research*, PIER 25, 39-50, 2000.

L. Zurk, K. Ding, L. Tsang and D. Winebrenner, “Monte Carlo Simulations of the Extinction Rate of Densely Packed Spheres with Clustered and Nonclustered geometries, *Digest IEEE International Symposium on Geoscience and Remote Sensing (IGARSS'94)*, Pasadena, USA, pp. 535-538, 1994.